

*Original paper***Part of Topical collection:  
“Advancements in Applied Geoinformatics”**

## Simplification of 2D shapes with equivalent rectangles

**Andrzej Kwinta<sup>1</sup>, Joanna Bac-Bronowicz<sup>2</sup>**<sup>1</sup>University of Agriculture in Krakow, Krakow, Polande-mail: [andrzej.kwinta@urk.edu.pl](mailto:andrzej.kwinta@urk.edu.pl); ORCID: <http://orcid.org/0000-0002-2003-7703><sup>2</sup>Wroclaw University of Science and Technology, Wroclaw, Polande-mail: [joanna.bac-bronowicz@pwr.edu.pl](mailto:joanna.bac-bronowicz@pwr.edu.pl); ORCID: <http://orcid.org/0000-0001-9038-1131>\*Corresponding author: Andrzej Kwinta, e-mail: [andrzej.kwinta@urk.edu.pl](mailto:andrzej.kwinta@urk.edu.pl)

Received: 2022-01-05 / Accepted: 2022-02-08

**Abstract:** Real objects in horizontal projection often have a complex geometry. Their irregular shape causes issues during analyses and calculations that consider their geometry. The paper proposes the replacement of real-world objects with equivalent rectangles (ER). The paper also defines the geometric criteria of ER as well as ER parameters and methods for calculating them. The paper also demonstrates the difference in the duration of calculations for different types of rectangles (equivalent rectangle with the same area, surrounding rectangle with the smallest area, inscribed rectangle with the largest area). The presented approach has been illustrated with three case studies. The first one is the application of ER to underground mining cavities to determine post-mining deformations of the ground surface. In the second study, an ER was applied to analyse the geometry of agricultural parcels in a selected part of a rural settlement. ER can help assess whether the spatial layout is faulty and if a planning intervention is necessary. The third example describes a building's geometry with an ER. Regarding the simplification of building's geometry, it is crucial to replace a simplified building with a model that has the same centroid location and the same area. It is the perfect solution for rapid analyses of displaying objects on maps in various scales.

**Keywords:** equivalent rectangle, geometry simplification, underground mining cavities, agricultural parcels, building geometry



The Author(s). 2022 Open Access. This article is distributed under the terms of the Creative Commons Attribution 4.0 International License (<http://creativecommons.org/licenses/by/4.0/>), which permits unrestricted use, distribution, and reproduction in any medium, provided you give appropriate credit to the original author(s) and the source, provide a link to the Creative Commons license, and indicate if changes were made.

## 1. Introduction

Analyses and calculations in various branches of economics often use representations of real-world objects (Müller et al., 1995; Liu et al., 2010). Such objects need to be described as precisely and accurately as possible, depending on the purpose and requirements necessary for the calculations. Taking into consideration the complexity of objects and requirements of computational models, we simplify real objects and replace them with geometric figures, the geometry of which can be determined easily (Kohl, 1850; Kwinta and Bac-Bronowicz, 2020). We also divide objects into two-dimensional and three-dimensional figures to calculate their area or volume (e.g. division of a parcel into triangles). It is possible to select basic two-dimensional figures in such a way that they precisely resemble the measured object (Bac-Bronowicz et al., 2009), for instance, the strips method for parcel area calculation (Maling, 2016).

The other issue is the replacement of complex real-world objects with simplified ones (described mathematically). The simplification of the object's geometry is fundamental in map generalisation in cartography (Buttenfield and McMaster, 1991). Depending on the type and shape of an object, various algorithms are applied to simplify its geometry (Mackaness et al., 2011). There are different approaches to area features (such as parcels or lakes) and linear features (such as rivers, roads, or borders) (Weibel, 1997; Chrobak et al., 2017). The simplification criteria are selected considering the most important attributes of a given feature (White and Renner, 1957; Gibbs, 1961).

In some instances, simplification is done not to visualise an object but to determine its geometry (Kosturbiec, 1972). Determination of the actual shape of an object is not a simple task (Bunge, 1966). It requires parametrisation. Stating that a given object is elongated and determining its length and width ratio is not unambiguous for real-world objects unless the object is a simple geometric shape. Often, the location of an object in the coordinate system or the direction of the main axis of the object are also crucial for such cases. The goal of simplification determines the choice of the generalisation method for a specific object.

Another issue is the arrangement of polygons in a rectangle (Alt et al., 2017). This problem concerns optimising the distribution of a fixed set of elements (their displacement and rotation) inside a smaller rectangle, for example, when cutting out parts from a metal sheet to minimise process waste.

In some cases, especially those concerning acceleration or simplification of calculations (based on an object's approximate geometry with the value of its area retained), a real object can be replaced with a simple figure, for example, a rectangle. If appropriate crucial criteria are introduced for given replacement conditions, the resulting figure can be considered an equivalent one.

One of the approaches to determining a feature's geometry is to transform an object into a simple geometrical shape, the parameters of which can be easily calculated. The simplest solution is to replace an object with a corresponding rectangle in many cases. It is because, for this figure, we can unambiguously determine axis directions as well as the geometric centre, length, width, and elongation. However, for most real-world objects, it is impossible to replace them directly with rectangles. In these cases, specific criteria of

transformation have to be followed. Moreover, the criteria for selecting a rectangle (e.g. the minimum bounding rectangle) for each object should be consistent and objective to ensure reproducible results.

The paper proposes a method for replacing an area feature (in this paper, homogeneous, simply connected objects) with an equivalent rectangle (ER). The criteria for considering a rectangle equivalent have been determined (section two). Steps of ER calculation have been presented. The speed of computations for an ER has been compared with the speeds of computations for other characteristic rectangles (section three). The focal point is differences in the duration of calculations for various types of rectangles. One has to keep in mind that replacing an object with an equivalent rectangle is not a generalisation of the object in cartographic terms.

Use of ERs makes it possible to determine geometric parameters of objects, which is necessary for various spatial analyses and calculations. It further facilitates the use of simplified rectangle geometry in computations.

The application of this approach is presented with three case studies. In the first one, it was used to simplify the geometry of forecasted post-mining cavities and the influence of such a simplification on determining land surface deformations. In the second case, the analysis concerns the shapes of agricultural land parcels, the transformation of which is important in agricultural land management and optimisation of agricultural production. The third example presents the replacement of a building's shape with different rectangles and a comparison of the real-world shape of the object with the ER in different map scales. Feature replacement with triangles has been known and widespread in topology and cartography. Their potential for other fields eludes the attention of various specialists. The authors of this article believe that it will be interesting for specialists from various industries, such as mining or agriculture. We used vector data in all the examples (coordinates of boundary points in local coordinate systems).

## **2. Determination of object's shape parameters**

Due to numerous natural and anthropogenic factors, the shapes and dimensions of various two-dimensional real-world objects (or their horizontal projections) are irregular (Koszturbiac, 1972). Such disadvantageous geometric shapes hinder analyses and calculations. That is why it is necessary to find shapes that may replace such objects (Bunge, 1966). The most important aspect of the issue is simplifying its geometry while retaining the most important geometric attributes of a given object. For two-dimensional objects, the simplest shape that might be used as a replacement in most cases is the rectangle.

The literature provides numerous studies on whether or not a given object is a rectangle and, in case it is not, how deformed it is (Rosin, 1999). What is more, various parameters could be used to assess the degree of rectangularity of an object (Hu, 1962; Peura and Iivarinen, 1997; Zandonadi et al., 2013).

Replacing every polygon with a rectangle entails selecting the appropriate optimisation solution for different analyses. There is no universal optimisation solution. Diverse

criteria should be developed for various applications in different sciences. We can choose one of the following criteria to describe the geometry of an object:

- surrounding rectangle with the smallest area, Minimum Bounding Rectangle (SR, MBR) (Smith and Chang, 1996; Chaudhuri et al., 2012);
- inscribed rectangle with the largest area, Maximum Empty Rectangle (LR, MER) (Molano et al., 2012; Sarkar et al., 2018);
- equivalent rectangle with the same area (ER) (Rosin, 2003; Kwinta and Gniadek, 2017).

In further considerations, we will focus on the equivalent rectangle method. Such rectangles are suitable for 2D objects for which their area is the most important factor. Real-world shapes of actual area features, often very complex, may be replaced by hypothetical rectangles. If a given rectangle meets established geometric criteria, it can be qualified as an equivalent rectangle. An equivalent rectangle should meet a selection of requirements concerning its geometry in reference to real objects. The following definition of an equivalent rectangle is introduced:

**Definition 1.** A rectangle is called an equivalent rectangle (ER) for any given simple connected 2D object, if:

- (a) the degree of overlap between the object and the ER is greater than the set criterion ( $q_{\min}$ );
- (b) the object's and the ER's centres of gravity coincide;
- (c) the longitudinal and transverse axes of both figures are collinear;
- (d) the area of the ER is equal to the area of the object.

The (a) requirement determines whether a given 2D object can be replaced with an equivalent rectangle. The remaining three requirements determine the ER's geometry. Figure 1 depicts the idea of an equivalent rectangle under Definition 1.

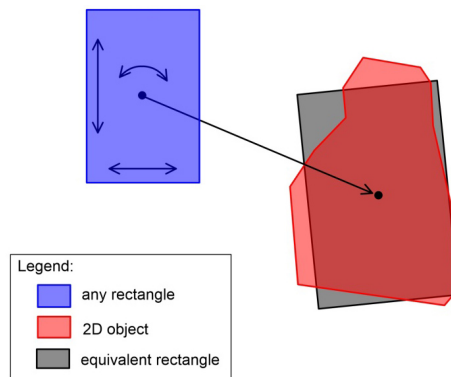


Fig. 1. Equivalent rectangle (ER) for a given object

The idea of ER is based on a series of transformations of a rectangle so that it meets the defined criteria. The possible transformations are presented in Figure 1; these are the changes of shape (ratio of sides), size (enlargement, reduction), and location (rotation, translation). In order to make such transformations and obtain an ER, it is necessary to conduct a series of calculations.

In theory, each and every object can be described as or replaced with a rectangle, but in some cases, for particular geometric objects, it would be pointless. Some objects cannot be properly described with a rectangle. For example, for letter-shaped objects, it is possible to circumscribe a rectangle on such an object, but due to the fact that the object has by no means the shape of an rectangle, such replacement of the object with an ER is doubtful. Figure 2 below presents an example of a few residential buildings situated in a housing estate in Wrocław. None of these buildings can be replaced with a rectangle, which is only logical because none of their shapes are even remotely similar to a rectangle. For such objects, the SR rectangle can be circumscribed, but this would not facilitate geometry description.

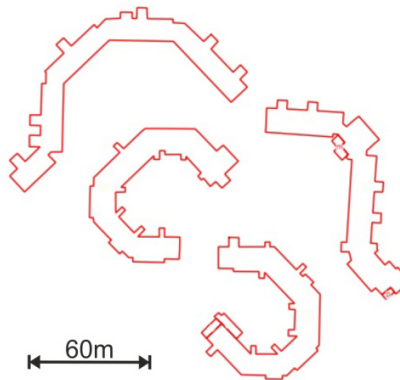


Fig. 2. Residential buildings situated in a housing estate in Wrocław

The most important factor in simplifying building geometry is the constancy of a building's centroid and the value of its area. Therefore, although an ER is the best solution to achieve such goals, note that not every building can be replaced with a rectangle. The calculation steps are presented in the next section.

### 3. Steps of ER calculation

To determine the basic geometric parameters of objects, we use the moments of inertia of two-dimensional geometric figures (Prokop and Reeves, 1992). As a result of several steps of calculations, the following parameters may be obtained:

- area ( $A$ )

$$A = \int_A dA \quad (1)$$

- geometric centre ( $C$ )

$$x_C = \frac{\int_A x dA}{A}, \quad y_C = \frac{\int_A y dA}{A} \quad (2)$$

- directions of transverse and longitudinal axes ( $\alpha_T, \alpha_L$ )

$$\alpha_L = \frac{1}{2} \arctan \left( \frac{2J_{0xy}}{J_{0x} - J_{0y}} \right), \quad \alpha_T = \alpha_L + 90^\circ \quad (3)$$

- elongation coefficient ( $e$ )

$$e = \frac{J_1}{J_2} \quad (4)$$

- lengths of ER sides ( $a, b$ )

$$\begin{cases} a = \sqrt{Ae} \\ b = \sqrt{\frac{A}{e}} \end{cases} \quad (5)$$

- degree of overlap ( $q$ )

$$q = 100\% - \text{DFS} = \frac{\int_A \delta(n) dA}{A} 100\% \quad (6)$$

where geometric moments of inertia (Hu, 1962; Pilkey, 1993):

- axis

$$\begin{aligned} J_x &= \int_A y^2 dA \\ J_y &= \int_A x^2 dA \\ J_{xy} &= \int_A xy dA \end{aligned} \quad (7)$$

- central

$$\begin{aligned} J_{0x} &= J_x - Ax_C^2 \\ J_{0y} &= J_y - Ay_C^2 \\ J_{0xy} &= J_{xy} - Ax_C y_C \end{aligned} \quad (8)$$

- main

$$\begin{aligned} J_1 &= \frac{J_{0x} + J_{0y}}{2} + \sqrt{\frac{(J_{0x} - J_{0y})^2}{2} + J_{0xy}^2} \\ J_2 &= \frac{J_{0x} + J_{0y}}{2} - \sqrt{\frac{(J_{0x} - J_{0y})^2}{2} + J_{0xy}^2} \end{aligned} \quad (9)$$

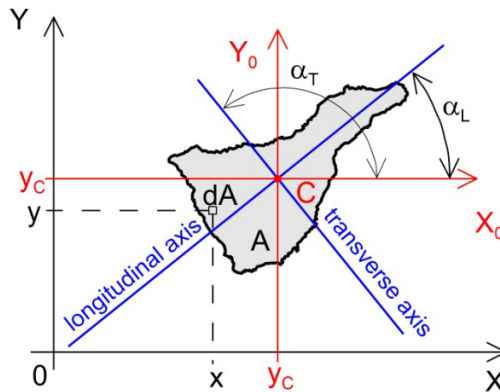


Fig. 3. Establishing the parameters of a 2D object

Figure 3 presents an object in a coordinate system. It also depicts some of the object's geometric parameters that could be calculated with equations (1)–(3) and (7)–(9).

The distortion factor of shape (DFS) (Rosin, 1999; Rosin, 2003; Kwinta and Gniadek, 2017; Kwinta and Bac-Bronowicz, 2020)

$$\forall_{n(x,y) \in A} \delta(n) = \begin{cases} 1, & n(x,y) \subset ER \\ 0, & n(x,y) \notin ER \end{cases} \quad (10)$$

$$\Delta A = A - \int_A \delta(n) dA \quad (11)$$

$$DFS = \frac{\Delta A}{A} 100\% \quad (12)$$

The optimal rectangle, in this case, means that the area of the object which does not align with the ER (Fig. 4) as a function of ER dimensions ( $a$ ,  $b$ ) and its angle of inclination in a coordinate system ( $\alpha_L$ ) amounts to the minimum.

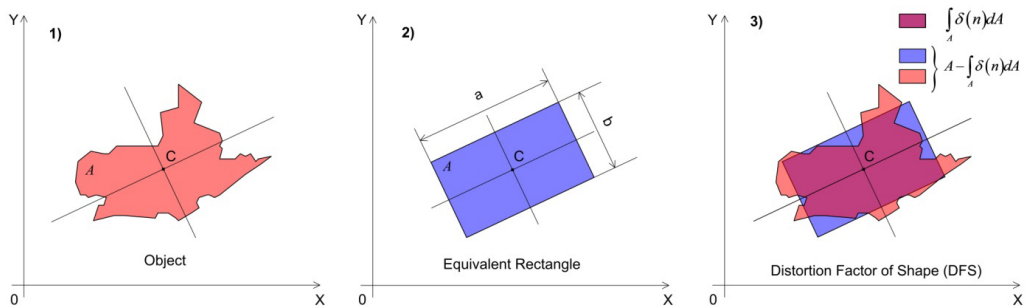


Fig. 4. Fitting an ER to an object: 1) Object, 2) Equivalent Rectangle, 3) Distortion

On the basis of the current experience of the authors, the following can be used as the threshold (minimal) value:

$$q_{\min} = 70\% \quad (13)$$

It is a subjective threshold, which facilitates the selection of objects with shapes significantly different from a rectangle. In the computational algorithm, each object that does not conform to this criterion should be analysed individually by the analyst, who would decide whether to continue the calculations or exclude the object from further analysis.

The above-mentioned theoretical considerations might be easily applied in a computer program or used as a GIS or CAD system procedure. The only computational difficulty is the calculation of integrals. However, all integrals can be calculated simultaneously (surface integrals of the analysed object). As a result, the outcomes can be obtained very quickly.

In general, when the smallest surrounding rectangle or the largest rectangle are being calculated, such rectangles have to meet the assumed minimising criterion. No other requirements for the rectangle's shape or location are set. The differences in calculation duration for different types of rectangles (ER, SR, and LR) will be discussed below. The same criteria have been employed in the analysis of all types of rectangles. These are the same elongation vector and centroid (which constitutes the essential requirements for sets harmonisation (INSPIRE, 2007)). Hence, the resulting rectangles (both LR and SR) are not optimal according to the minimisation criterion.

The calculation steps are the same for different types of rectangles. If parameters of the object are known, the determination of the smallest surrounding rectangle is a trivial issue since it requires simply the calculation of the minimal and maximal coordinates of the object in the coordinate system, where the object's elongation is aligned with the x-axis. It is necessary to apply the iterative method to calculate the largest rectangle.

The analysis is conducted for an equivalent, the smallest surrounding, and the largest rectangles. For this purpose, special rectangle-generating software with a timer for computing has been prepared. The beginning of calculations is the same for all three types of rectangles (classic calculation of the moment of inertia). The next stage of the calculations for all rectangles is the introduction of a local coordinate system with its origin in the object's centre of gravity and with the axis in line with its vectors of main inertia moments.

The calculation of the equivalent rectangle consists of using formulas 1–3. Next, when the lengths of its sides and centre are determined, the coordinates of ER vertices can be calculated.

The calculation of the smallest surrounding rectangle is connected with finding the largest coordinates of the object in the local coordinate system. The coordinates constitute half of SR's sides. Then the coordinates of the SR vertices can be calculated.

The most complex case is the calculation of the largest rectangle. This task has been done iteratively. In order to determine the LR, the longest and the shortest distances from the object's centre of gravity to its edge have been computed. These distances constitute



half of the LR's diagonal. Next, the rectangle of the largest area, the sides of which do not cross the object's sides (but tangency is allowed), is sought between these largest and smallest values using the iterative method.

The comparative analysis of the calculation duration has been conducted for four objects. The objects were four islands: Fuerteventura, Jamaica, Sri Lanka, and Taiwan. All three types of rectangles have been calculated for each object. The outcomes of the calculations of geometric parameters and the duration of calculations are presented below in Table 1. Table 2 shows sizes of the rectangles and the percentage differences between areas of the islands and areas of the rectangles.

Table 1. The geometric parameters of islands and duration of calculations

Island	Vertexes	Island geometry			Time of calculation (msec)		
		$A$ ( $\text{km}^2$ )	$e$	$\alpha_L$ ( $^\circ$ )	ER	SR	LR
Fuerteventura	200	1.66	2.91	57.2	0.166	4.88	6609.0
Sri Lanka	333	65.78	1.80	99.8	0.174	8.13	11216.0
Taiwan	435	35.95	2.66	71.0	0.167	10.28	15047.0
Jamaica	540	10.91	3.10	170.0	0.170	12.88	18456.0

Table 2. Sizes of different kinds of rectangles

Island	Equivalent Rectangle			Smallest Rectangle			Largest Rectangle		
	$a$ (km)	$b$ (km)	$q$ (%)	$a$ (km)	$b$ (km)	$\Delta A$ (%)	$a$ (km)	$b$ (km)	$\Delta A$ (%)
Fuerteventura	69.6	23.9	76.2	112.6	40.0	170.9	40.0	15.3	-63.1
Sri Lanka	344.2	191.1	88.8	466.2	243.9	72.9	269.2	125.5	-48.6
Taiwan	309.5	116.2	88.8	397.9	153.8	70.2	241.7	83.2	-44.0
Jamaica	183.9	59.3	82.3	243.0	94.0	109.4	93.3	45.5	-61.1

Considering the results of the calculations in this example, the shortest computation time was recorded for the ER. For the SR, this time was around 50 times longer, and for the LR, around 10 000 times longer. As shown in Table 1, the computation time for the ER is more or less constant, even for objects with more vertices. On the other hand, for the SR and the LR, the number of vertices has a significant impact on the duration of calculations; as the number of vertices increases, the computation time increases as well. Undoubtedly the computation time depends on the parameters of the computing device and may vary significantly for different computers. Regardless of the computer used, the trend is unchanged, and the ER calculation is the fastest one.

The results of the calculations are visualised in Figure 5. The following sections present different applications of ERs in various scientific fields.

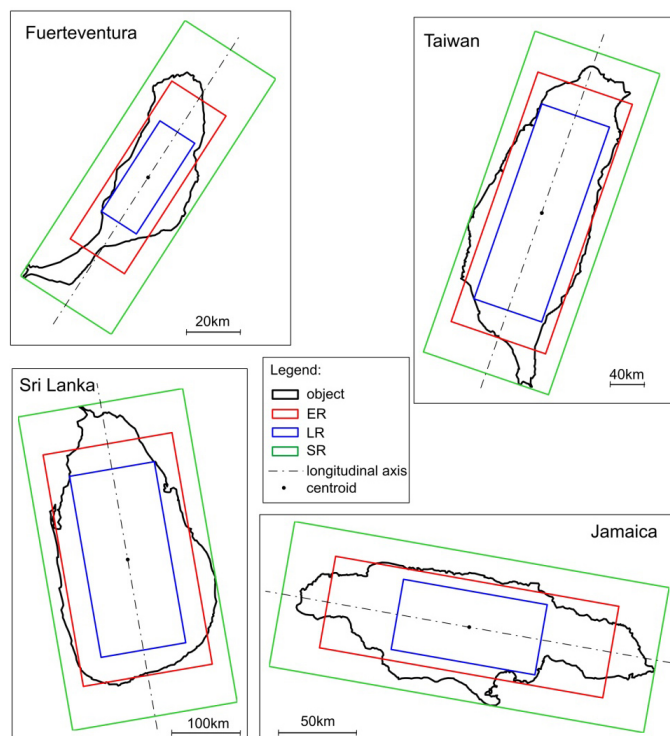


Fig. 5. Objects and respective ER, SR, and LR

#### 4. Mining extraction – a case study

This example is not a typical determination of an object's geometry but rather focuses on replacing real-world geometry with ERs.

Underground mineral extraction creates hollow spaces in the rock mass, which migrate upwards and result in relocations and deformations of the surface (Peng, 1986). The optimal form of mining is selected depending on the mining and geological conditions of the mineral bed. Forecasting terrain deformations caused by ongoing mining operations is a vitally important issue, crucial for proper mining planning (Kratzsch, 1983; Kwinta and Gradka, 2018; Kwinta and Gradka, 2020). Theoretical calculations of the deformation index use computational models (Chugh et al., 1989). Currently, the geometric-integral and geo-mechanical models are the most commonly used methods for such theoretical calculations (Bahuguna et al., 1991). Figure 6 presents the operational principle of a group of theoretical models based on the influence function (Díaz-Fernández et al., 2010; Li et al., 2018). The elementary void  $dV$  is moving throughout the rock mass to the terrain surface. The void's movement and the effect of such a movement on the terrain surface, which is the elementary subsidence, can be described using the influence function  $f$ . The shape of the subsidence on the terrain surface can be determined by summing up the movements of all voids.

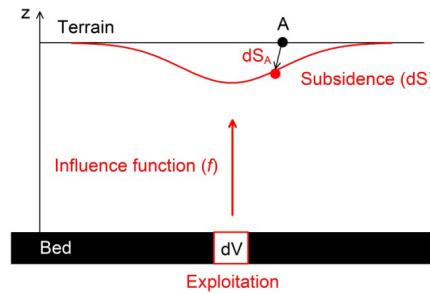


Fig. 6. The influence function

Through the influence function  $f$ , the elementary excavation  $dV$  (cause) at point  $P$  generates the elementary subsidence  $dS$  (effect):

$$dS_P = f(X; k) dV \quad (14)$$

where  $dS_P$  – the elementary subsidence of point  $P$ ,  $f(X; k)$  – the  $f$  is the influence function, the  $X$  is the set of geometric data, and the  $k$  is the set of model parameters,  $dV$  – the elementary excavation volume.

By adding elementary influences from all elements of the excavation with the use of an integral (Peng, 1986; Kratzsch, 1983), one can calculate the subsidence. The total subsidence of point  $P$  is:

$$S_P = \iint_A f(X; k) g dA \quad (15)$$

because  $dV = g dA$  – the element volume is a product of thickness ( $g$ ) and area ( $dA$ ).

The accuracy of the calculation results leans firstly on the correct description of the excavation geometry (especially its volume because we calculate influences with the surface integral) and secondly on the adopted parameters of the theoretical model that are suitable for particular geological and mining conditions.

Depending on the type of mineral and mining system, post-mining voids might have regular (wall system) or irregular (cavity system) shapes (Hejmanowski et al., 2018). For example, Figure 7A presents a set of mining cavities in an underground salt mine marked in grey. These are 301 mining cavities located from 60 to 300 meters under the surface. The cavities have various floor sizes (from 6 m<sup>2</sup> to 6 000 m<sup>2</sup>, the average of 624 m<sup>2</sup>) and are described using various numbers of vertices (from 4 to 56, the median of 19).

Calculations of deformation factors are considerably time-consuming, especially for a large number of surface points (more than 100 000 points, for example) and for numerous time horizons (for example, salt rock mass deformations have been forming even up to 100 years). Deformations are calculated for each cavity, for each point, and in each time horizon. The computation process is very time-consuming. It may be accelerated through the simplification of the excavation geometry. However, it has to be done so as not to impact the values of deformation. ER generated for mining cavities geometry are marked in light red in Figure 7B.

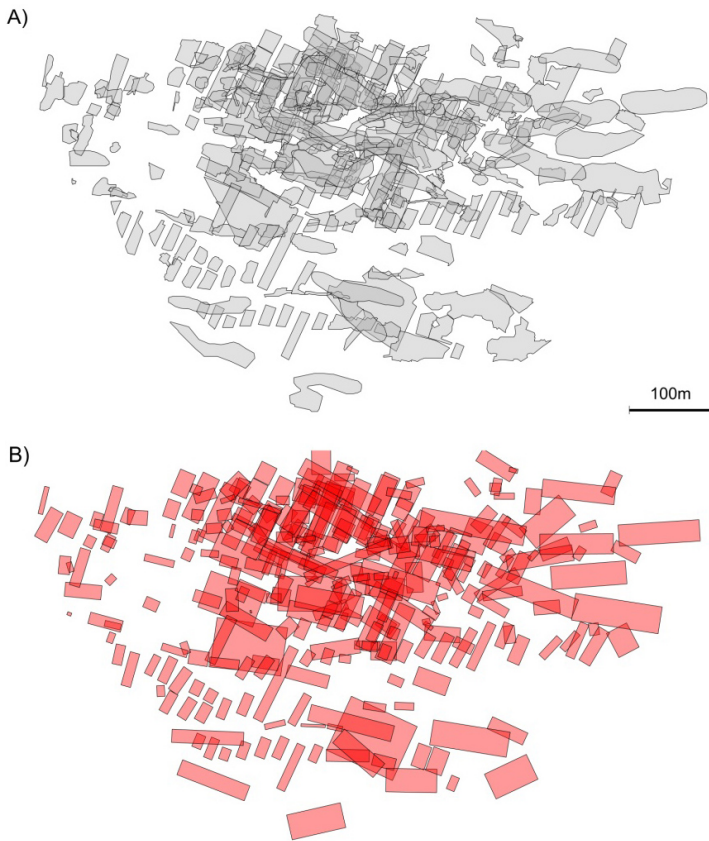


Fig. 7. Outline of distribution of A) mining cavities and B) ERs

The forecast terrain subsidence within the area of excavations was determined using the MODEZ 4.0 mining deformation prediction system (Hejmanowski and Kwinta, 2010) based on the modified Knothe theory (the geometric-integral theory) for the actual shapes of the excavations and for cuboids based on ERs for the excavations.

Figure 8 presents the results of subsidence calculations for the entire geometry (A). The results obtained in both processes (real-shaped cavities compared with ERs) differed less than 15 mm (B), which is not significant in this case (the maximum subsidence is 2 146 mm). Nevertheless, the computation time was reduced considerably. In this example (301 cavities, 4000 points, 2 time horizons) the original cavity data calculation took 45 minutes; for ER, the calculation took 29 minutes.

Therefore, it can be concluded that the change of the shape of cavity floor into ERs did not cause significant changes in the forecasted deformation indicators, whilst the computation time decreased noticeably. Hence, such a simplification can be introduced for this group of cases. However, each case should be approached individually. Furthermore, appropriate analyses should be performed before applying this solution (whether each cavity can be replaced with a rectangle).

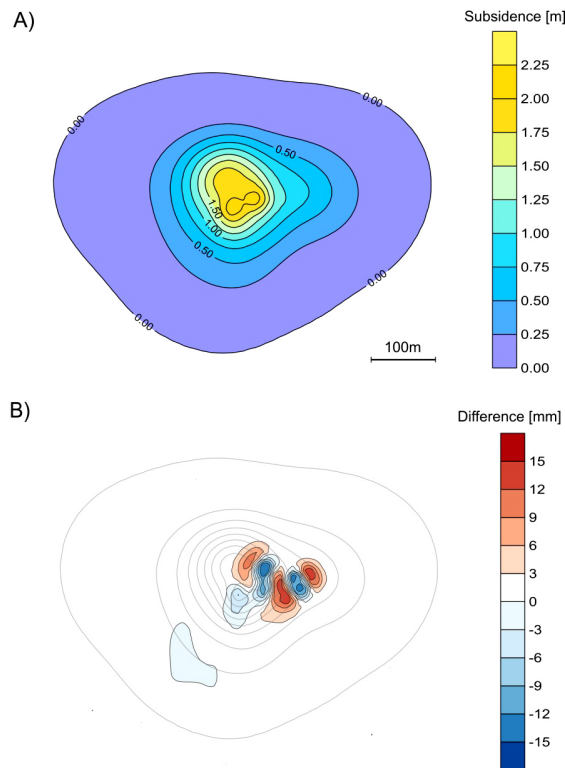


Fig. 8. Results of subsidence forecast A) terrain subsidence (m) and B) subsidence difference (mm)

## 5. Agricultural parcels – a case study

Proper configuration and situation of parcels in an agricultural holding are primary conditions for effective production (Hartvigsen, 2014). Throughout the years, the spatial structure of an agricultural holding depended on numerous factors, which greatly influenced the final layout of fields in the rural landscape. Both land transactions and the division of inherited land led to an increase in the number of new parcels with declining spatial parameters (Demetriou et al., 2013). The abnormalities in the spatial structure of land, increasing over time, hurt the farming process and resulted in the need for land consolidation to improve the structure (King and Burton, 1982; Manjunatha et al., 2013; Hanus et al., 2018; Len, 2018). This problem is widely known all around the world.

In order to optimise the agricultural activity within a holding, it is necessary to determine several parameters encompassing its full characteristic, including the geometry of parcels, among other things. A number of parameters relevant to faulty spatial structures were developed (Janus and Taszakowski, 2015). Among the parameters describing parcel geometry, the crucial ones for agricultural productivity are the parcel's size and shape. Particularly important is its elongation and the elongation direction in relation to the terrain gradient and sunlight direction.

The use of ERs in the analysis of parcel shape facilitates the quick identification of defective structures and determination of the general direction of necessary changes (consolidation, division, shape modification).

An example of the agricultural application of ER is the description of parcel geometry in a rural settlement in southern Poland. Data on 892 land parcels were collected, shown in grey in Figure 9A. Roads, parcels with the  $q$  parameter lesser than 70% (13), and small parcels with an area lesser than 1000 m<sup>2</sup> were rejected (324 parcels rejected in total). We calculated ERs for specific parcels using software consistent with the solutions presented in the second section (Fig. 9B). With ER, it is easy to analyse the shapes of individual parcels. Thanks to the employed parameters, it was possible to determine whether it was necessary to consolidate land in a given region or whether the structure had to be transformed to increase agribusiness efficiency (providing data for detailed analyzes).



Fig. 9. Outline of parcels' situation (A) and their equivalent rectangles (B)

Table 3 presents the extreme and average values of parcel parameters. The data in Table 3 show that the layout of parcels in the analysed village was satisfactory. The mean degree of overlap is 91.17%. The average ratio of the longer and shorter side was 6.46.

Table 3. Parameters of the analysed parcels

Parameter	Vertexes	$A$ (m <sup>2</sup> )	$\Delta A$ (m <sup>2</sup> )	$q$ (%)	$\alpha_L$ (°)	$a$ (m)	$b$ (m)	$e$
min	4	1001.40	3.30	70.38	1.98	33.84	7.42	1.04
mean (median*)	11*	3140.96	301.65	91.17	68.41	129.41	25.48	6.46
max	33	19899.94	2817.22	99.77	183.16	363.07	110.13	30.46

Another interesting application of the proposed approach may be the analysis of the directions of parcel elongation ( $e$ ) in relation to the directions of the maximum terrain slope. This information is crucial for water soil erosion. The subject has been studied for over a hundred years in Poland, and the precursor of such studies was the agro-meteorologist Bac (1928). Currently, the issue is broadly studied (Józefaciuk and Józefaciuk, 1987; Woch, 2008; Wawer and Nowocien, 2018). Figure 10 presents the vector difference between the maximum slope of parcels and their elongation as a function of the mean slope angle for each parcel.

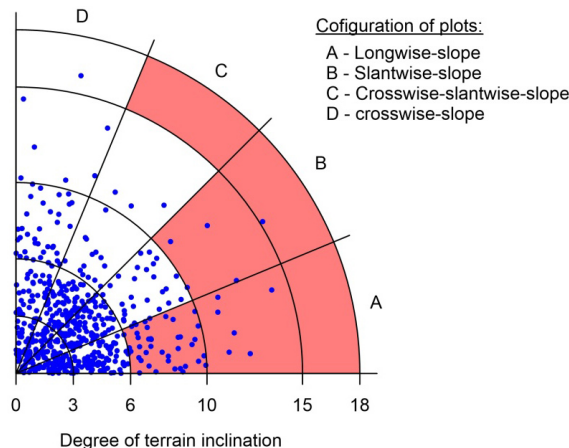


Fig. 10. Elongation and configuration of parcels as a function of terrain slope

When designing the consolidation process for many different places, it is important to counteract the damages caused by water erosion (Wawer and Nowocien, 2018). Therefore, the appropriate reshaping of agricultural parcels depends on water erosion risk and is very important (Woch, 2008). The literature offers analyses of the appropriate layouts of parcels (vector) and their sizes, depending on the level of water erosion risk. The replacement of virtual parcels with ER facilitates quick analysis of this issue. The maximum slope of parcels and the direction of this slope can be determined with a numeric terrain model. The pie chart in Figure 10 shows individual parcels (blue points) with the values of their slopes (radii of sectors reflect water erosion risk caused by the slope) and the vector difference between the parcel's elongation and its maximum slope (divided into four sectors related to parcel arrangement). The sectors in red are those for which water erosion may be a severe threat. Therefore, all parcels assigned to these sectors need to be thoroughly analysed (Józefaciuk and Józefaciuk, 1987; Woch, 2008).

Replacement of parcels with ERs facilitates a quick spatial analysis of rural settlements, it can also help assess whether the spatial layout is faulty and if a planning intervention is necessary (Woch, 2008; Kwinta and Gniadek, 2017). We do not use this solution straightforward. In the real-world scenarios, we do not automatically convert parcels into rectangles. In this case, the ER is only a tool for obtaining geometric data for further analyses and detailed work.

## 6. Structure – case study

The data included in geoinformation systems are obtained in different ways (Bac-Bronowicz et al., 2009; Bielecka, 2015), based on land surveys or multispectral satellite or airborne imagery (Huertas and Nevatia, 1988). They are also obtained from historical sources, paper maps or digital resources (Ghaffarian, 2014; Bac-Bronowicz et al., 2016).

Regarding the simplification of object's geometry, it is crucial to replace a simplified object with a model that has the same centroid location and the same area. In such cases, the best approach is to employ the ER.

Furthermore, in the case of structures, it is necessary to determine their geometric parameters, which is not an easy task due to the significant diversity of architectural solutions. In the case of complex shapes of buildings or structures that are not simply connected figures in the horizontal projection, the result of such an analysis might be misleading. The object should then be divided into modules (with simple geometry). Figure 11 presents a historic building from the 14<sup>th</sup> century, St. Elizabeth's Church located near the Wroclaw Market Square in Poland with calculated rectangles (minimal, maximal, and equivalent).

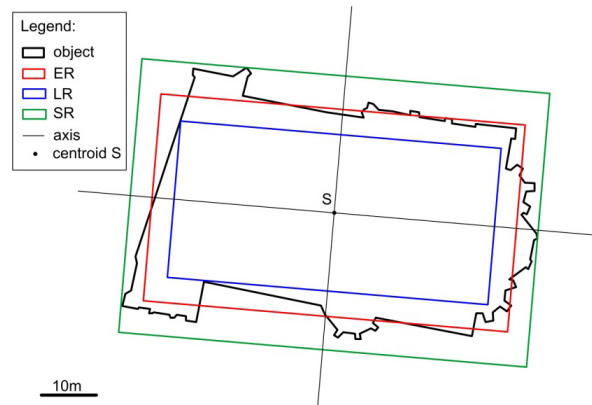


Fig. 11. The contour of St. Elizabeth's Church, Wrocław and rectangles

During the process of the ER calculation, basic parameters of the object were calculated (area, length of walls, geometric centre, angle of the longitudinal and transverse axis rotation). Since the object is irregular (note the steeple), the longitudinal axis (the thin black line visible in Figure 11) does not align with the axis of the nave. The degree of the ER's overlap is 93.1%. Hence it can be stated that the ER is correctly fitted to the object.

For comparison, LR and SR were also determined. For all the rectangles (ER, SR, LR), the basic assumption was that the axes and centroid had to overlap with the axes and centroid of the object (Bac-Bronowicz et al., 2010). When analysing the results shown in Figure 11, it should be noted that the calculated SR marked in green meets the assumptions, but it is not the smallest possible rectangle. A similar observation applies



to the LR marked in blue in Figure 11. The axes of this rectangle and its centroid are the same as for the object, but this is not (generally) the largest rectangle. The dimensions of the rectangles and their areas are listed below in Table 4.

Table 4. Dimensions of the rectangles

Object	Length (m)	Width (m)	Area (m <sup>2</sup> )
ER	66.90	37.98	2540.86
SR	74.90	50.24	3762.98
LR	58.85	28.70	1689.00

The issue of cartographic simplification of the geometry of area and linear features has been deeply analysed in the literature (Mackaness et al., 2011; Chrobak et al., 2017). Using the ER, we do not create a generalisation, but we convert a given object into a rectangle. Let us assume that the decision to replace a 2D object with an ER is related to the significance of this object and the visual aspect of the problem for a given imaging scale. If (for a given object visualisation scale) the mean distances between the object's edges and the ER are unrecognisable for the observer, then the object can be replaced with an ER.

The recognition of the distance between two elements is related to the angular resolution of the observer's sight (Salishchev, 1976). For example, in classical cartography, the minimum distance between two parallel linear features can be distinguished in millimeters. In the case of digital imaging, this distance is related to the screen resolution and is expressed in pixels. To illustrate the visibility of objects on the screen, Table 5 shows the minimum dimensions of recognisable objects.

Table 5. Dimensions of recognisable objects displayed on a screen

Recognizability	1 pixel = 0.26458 mm		2 pixel = 0.52916 mm	
	Length (m)	Area (m <sup>2</sup> )	Length (m)	Area (m <sup>2</sup> )
500	0.13	0.0175	0.26	0.0700
1000	0.26	0.0700	0.53	0.2800
2000	0.53	0.2800	1.06	1.1201
5000	1.32	1.7501	2.65	7.0003
10000	2.65	7.0000	5.29	28.0010
25000	6.61	43.7516	13.23	175.0060
50000	13.23	175.0064	26.46	700.0258

Let us denote the minimum distance by symbol  $d_m$ . The minimum resolution for classic images can be assumed to be 0.3 mm according to the Salishchev norms for drawing recognisability (Salishchev, 1976), while for digital images, it is 1 pix (Baranska et al., 2021).

The issue of an object's importance can be resolved by assigning objects to specific categories. Let us assume that we can assign objects to 10 categories of importance. The lowest is 1, and the highest is 10. Let us denote the category number  $K$ . We can propose the following relationship for the importance coefficient  $k_i$  to be used in the graphs:

$$k_i = \left( \frac{5}{10 - K} \right)^2 \quad (16)$$

The value of the importance coefficient defined above equal to 1 corresponds to the average importance category ( $K = 5$ ); lower values mean less importance and values greater than 1, greater importance. For the  $K = 10$  category, the coefficient equals infinity.

Let us assume the relationship for the average distance between object edges and an ER for a given imaging scale:

$$d_s = \left( \frac{\Delta A}{4(a + b)M} \right)^2 \quad (17)$$

where  $a, b$  – the lengths of the ER sides (5),  $\Delta A$  – the difference in areas between the object and its ER (11) (Figure 4),  $M$  – the imaging scale.

If we know the importance coefficient  $k_i$  (16) and the mean distance  $d_s$  (17), then, by introducing the minimum recognisable distance, we can establish the criterion of substitution as follows:

$$k = \begin{cases} 1 & k_i \cdot d_s \leq d_m \\ 0 & k_i \cdot d_s > d_m \end{cases} \quad (18)$$

where  $k$  – the criterion of substitution (1 – substitution, 0 – no substitution),  $d_m$  – the minimum recognisable distance (Salishchev, 1976; Baranska et al., 2021),  $k_i$  – the importance coefficient (16),  $d_s$  – the average distance between object's edges and the ER (17).

Now, let us illustrate this with an example. Figure 12 shows a comparison of the actual shape of the building (St. Mary's Basilica in Krakow, an old-town building listed by the UNESCO) with its ER in various imaging scales. First, the ER was calculated based on the geometric data of the object. Then, in accordance with the relationship (16)–(18), the criteria for substitution with the ER were determined, assuming an image resolution of 0.3 mm.

Data included in this example:

$$\begin{aligned} A &= 2526.18 \text{ m}^2 \\ \Delta A &= 367.3 \text{ m}^2 \\ a &= 75.16 \text{ m} \\ b &= 33.60 \text{ m} \\ d_m &= 0.3 \text{ mm} \end{aligned}$$

Depending on the map scale  $M$  and the importance of object  $K$ , its contours can be represented directly or replaced by an ER. According to the results, assuming the average

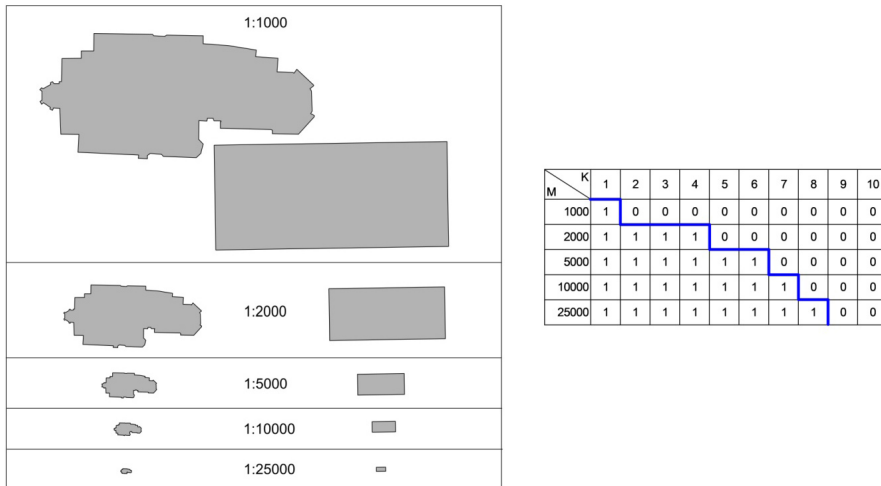


Fig. 12. Comparison of the shape of the structure and the ER depending on the map scale; the importance index  $k_i$  as a function of map scale  $M$  and importance factor  $K$

importance of the object for the scale of 1:5 000, the object's contours can be replaced with its ER. Similar calculations can be performed for digital imaging, determining whether the object's contour or its ER will be displayed on the screen. An additional advantage of this solution is the avoidance of "desert fog" (Touya, 2019) when changing the display scale of the object. Obviously, there is a lower limit to the application of the criterion of substitution. When the area of an object in a given imaging scale is too small (for example, Table 5), it is pointless to replace the object with an ER, and an appropriate cartographic symbol should be used.

## 7. Summary

It is often necessary to identify the geometric attributes or simplify the geometry of real-world area features. This is because they come in complex shapes, which often are difficult to describe unambiguously. Therefore, it is necessary to introduce certain simplifications to determine the geometry of such objects.

The significant attributes of 2D area features are their area, length of edges, distribution, and shape. Obtaining some of that information is easy based directly on the geometry of an object defined by the coordinates of its vertices. However, certain attributes are not directly available, and it is necessary to calculate them. In many fields of science, real objects are replaced with rectangles. One can search for the largest empty rectangle inside the object's borders (LR, MER) or the smallest one outside (SR, MBR). In many cases, these extreme rectangles do not have a common centroid with the object, and their axes differ as well. It results from various minimisation criteria because the criteria depend on the selected calculation goal. It is not the case when replacing a real object

with an ER defined in section 2 of the paper. In such a case, it is crucial to determine the necessary criteria for such an ER in order for it to represent the geometry of the real-world object accurately. What is most often required for both the object and the ER are the alignment of geometric centres, directions of moments of inertia, and the same area. The ER created in such a way may be used to analyse the object's geometry. The ER is an approximation of shape simplification, which can be used in specific generalisation tasks for high-frequency objects that do not require high accuracy. Still, it is necessary to retain their location and area.

Obviously not every ER depicts an object's geometry correctly. In such cases, the decisive factor is the degree of overlap  $q$  (or distortion factor of shape in relation to the rectangle, DFS).

The replacement of real-world objects with ERs can be used in calculation practice. The object's area is a crucial parameter in analyses within various scientific fields. The paper presents three different practical cases in which objects were replaced by equivalent rectangles.

The first case concerns simplifying the shape of underground mining excavation and assessing the impact of such simplification on the predicted land subsidence. As a result of calculations for ERs and cavities, it was demonstrated that the results were similar for both scenarios. Rock mass properties and excavation geometry are equally important for predicting deformations.

Next, the authors analysed the possibility of replacing agricultural parcels with ERs. In this case, geometric parameters of parcels and their deviation from the rectangular shape are crucial.

By replacing parcels with ERs, it was possible to obtain geometric parameters facilitating the analysis of the structure of the parcels. This helps make the decision concerning land consolidation or other projects (such as assessing the risk of erosion). In addition, information obtained by determining ERs may serve as a basis for assessing the formation of rural land layouts.

Finally, in the last example, the authors presented the possibility of ER application to quick simplification of buildings. A model of an object has been created using an ER conforming to parameters defined in the paper. The model is rectangular and has the same centroid, area, and elongation direction. Therefore, it is the perfect approach for rapid analyses of displaying objects on maps in various scales.

Based on the analysis of the presented examples, the following observations can be drawn:

- one can effectively replace homogeneous, simply connected 2D objects with equivalent rectangles;
- equations with moments of inertia give quick solutions;
- one can describe mining cavity geometry for deformation prediction using ERs;
- the introduction of the ER facilitates the assessment of the shape of agricultural parcels;
- using such geometric parameters of the ER as direction and slope simplifies the water erosion risk analysis in rural areas;
- the introduction of ERs to replace objects on maps simplifies fast visualization.

The paper presents an analysis of the computation time needed for different rectangles. Calculations of the equivalent, the largest, and the smallest surrounding rectangles have been performed using four islands as input data. The islands have different sizes and shapes and many boundary points. The calculations of the ERs were the most time effective, whereas the computations for the SRs were several dozen times slower. An LR was calculated even over 10 000 times slower (depending on the criteria of stopping the iterative procedure). Obviously, these discrepancies can vary for objects of different shapes, but the ER calculations are always the fastest.

All calculations conducted in the paper were made with original software specially created for the project. Further development of the software is planned for the future. The main development direction will be replacing real-world objects with simple geometric shapes (such as regular polygons).

### Author contributions

Conceptualization: A.K.; Methodology development: J.B.B.; Software development: A.K.; Data collection and analyses: A.K. and J.B.B.; Writing and editing: A.K.; Review and editing: J.B.B.

### Data availability statement

Section 2, 5, 6 – data obtained on the basis of the National Polish Geoportal – [www.geoportal.gov.pl](http://www.geoportal.gov.pl), Section 3 – data obtained from the Google Earth Pro application, Section 4 – data required to reproduce these findings cannot be shared.

### Acknowledgements

This research study has not received any external funding.

### References

- Alt, H., de Berg, M., and Knauer, C. (2017). Approximating minimum-area rectangular and convex containers for packing convex polygons. *J Comput. Geom.*, 8(1), 1–10. DOI: [10.1007/978-3-662-48350-3\\_3](https://doi.org/10.1007/978-3-662-48350-3_3).
- Bac, S. (1928). Contribution to research on the change in the position of arable loess soils. *Rocz. Nauk Rol. i Leś.*, 19(3), 463–499. Poznań.
- Bac-Bronowicz, J., Dygaszewicz, J., and Grzempowski, P. (2009). Contribute data from cadastral database to multiresolution topographic database. *Geomat. Environ. Eng.*, 3(1/1), 45–58.
- Bac-Bronowicz, J., Dygaszewicz, J., Grzempowski, P. et al. (2010). Reference databases as a source of power and updating of building layers in a multi-resolution topographic database. *Annals of Geomatics*, VIII, 5(41). Warszawa.

- Bac-Bronowicz, J., and Wojciechowska, G. (2016). The status of work on development of the database of architectural industrial heritage in Wrocław. *Annals of Geomatics*, 14(5), 537–548.
- Bahuguna, P.P., Srivastava, A.M.C., and Saxena, N.C. (1991). A critical review of mine subsidence prediction methods. *Min. Sci. and Technol.*, 13, 369–382.
- Baranska, A., Bac-Bronowicz, J., Dejaniak, D. et al. (2021). Unified Methodology for the Generalisation of the Geometry of Features. *ISPRS Int. J. Geo.-Inf.*, 10(3), 107.
- Bielecka, E. (2015) Geographical data sets fitness of use evaluation. *Geodetski Vestnik*, 59(2), 335–348.
- Bunge, W. (1966) Theoretical geography. Royal University of Lund. Dept. of Geography; Gleerup.
- Buttenfield, B., and McMaster, R. (1991). *Map Generalization: Making Rules for Knowledge Representation*. Longman: London.
- Chaudhuri, D., Kushwaha, N. K., Sharif, I. et al. (2012). Finding best-fitted rectangle for regions using a bisection method. *Mach. Vis. Appl.*, 23(6), 1263–1271. DOI: [10.1007/s00138-011-0348-6](https://doi.org/10.1007/s00138-011-0348-6).
- Chrobak, T., Szombara, S., Koziol, K. et al. (2017). A method for assessing generalized data accuracy with linear object resolution verification. *Geocarto Int.*, 32(3), 238–256. DOI: [10.1080/10106049.2015.14133721](https://doi.org/10.1080/10106049.2015.14133721).
- Chugh, Y.P., Hao, Q.W., and Zhu., F.S. (1989). *State of the art. in mine subsidence prediction*. In “Land Subsidence 1989” Publ. Balkema.
- Demetriou, D., Stillwell, J., and See. L. (2013). A new methodology for measuring land fragmentation. *Comput. Environ. Urban Syst.*, 39, 71–80. DOI: [10.1016/j.compenvurbsys.2013.02.001](https://doi.org/10.1016/j.compenvurbsys.2013.02.001).
- Díaz-Fernández, M.E., Álvarez-Fernández, M.I., and Álvarez-Vigil, A.E. (2010). Computation of influence functions for automatic mining subsidence prediction. *Comput. Geosci.*, 14(1), 83–103. DOI: [10.1007/s10596-009-9134-1](https://doi.org/10.1007/s10596-009-9134-1).
- Ghaffarian, S. (2014). Automatic building detection based on supervised classification using high resolution Google Earth images. *The International Archives of Photogrammetry. Remote Sens. Spatial Inf. Sci.*, 40(3), 101–106. DOI: [10.5194/isprsarchives-XL-3-101-2014](https://doi.org/10.5194/isprsarchives-XL-3-101-2014).
- Gibbs, J.P. (1961). *Urban research methods*. New York.
- Hanus, P., Peska-Siwik, A., and Szewczyk, R. (2018). Spatial analysis of the accuracy of the cadastral parcel boundaries. *Comput. Electron. Agric.*, 144, 9–15. DOI: [10.1016/j.compag.2017.11.031](https://doi.org/10.1016/j.compag.2017.11.031).
- Hartvigsen, M. (2014). Land reform and land fragmentation in Central and Eastern Europe. *Land Use Policy*, 36, 330–341.
- Hejmanowski, R., and Kwinta, A. (2010). Modeling continuous deformation of terrain in variable conditions of deposition. *Mineral Resources Management*, 26(3), 141–153.
- Hejmanowski, R., Malinowska, A., Kwinta, A. et al. (2018). *Modeling of land subsidence caused by salt cavern convergence applying Knothe’s theory*. Prace Instytutu Mechaniki Górotworu PAN (Transactions of the Strata Mechanics Research Institute), 20(2), 87–94.
- Hu, M.K. (1962). Visual pattern recognition by moment invariants. computer methods in image analysis. *IEEE Trans. Inf. Theory*, 8, 179–187. DOI: [10.1109/TIT.1962.1057692](https://doi.org/10.1109/TIT.1962.1057692).
- Huertas, A., and Nevatia, R. (1988). Detecting buildings in aerial images. *Computer Vision. Graphics. and Image Processing*, 41(2), 131–152.
- INSPIRE (2007). *Directive 2007/2/ EC of the European Parliament and of the Council of 14 March 2007*. Known as the INSPIRE Directive.
- Janus, J., and Taszakowski, J. (2015). The idea of ranking of setting priorities for land consolidation works. *Geomatics. Landmanagement and Landscape. Publ. University of Agriculture in Krakow*, 1, 31–43.
- Józefaciuk, Cz., and Józefaciuk, A. (1987). Study on anti-erosion utilization system of utilization of agricultural lands on upland areas. *Soil Science Annual*, XXXVIII, 1, 59–76.

- King, R., and Burton, S. (1982) Land fragmentation: notes on fundamental rural spatial problem. *Progress in Human Geography*, 5(6), 475–494.
- Kohl, J.G. (1850). *Der Verkehr und die Aussiedlungen der Menschen in ihrer Abhängigkeit von der Gestaltung der Erdoberfläche*. Leipzig.
- Kosturbiec, B. (1972). Analysis of concentration phenomena in settlement network. *Polish Academy of Sciences. Geographical Studies*, 93.
- Kratzsch, H. (1983). *Mining Subsidence Engineering*. New York: Springer-Verlag Berlin Heidelberg.
- Kwinta, A., and Gniadek, J. (2017). The description of parcel geometry and its application in terms of land consolidation planning. *Comput. Electron. Agric.*, 136, 117–124. DOI: [10.1016/j.compag.2017.03.006](https://doi.org/10.1016/j.compag.2017.03.006).
- Kwinta, A., and Gradka, R. (2018). Mining exploitation influence range. *Nat. Hazard*, 94(3), 979–997.
- Kwinta, A., and Bac-Bronowicz, J. (2020). Regular polygons in 2D objects shape description. *Geomatics. Landmanagement and Landscape*, 4, 43–61.
- Kwinta, A., and Gradka, R. (2020). Analysis of the damage influence range generated by underground mining. *Int. J Rock Mec.*, 128, 104263.
- Len, P. (2018). An algorithm for selecting groups of factors for prioritization of land consolidation in rural areas. *Comput. Electron. Agric.*, 144, 216–221. DOI: [10.1016/j.compag.2017.12.014](https://doi.org/10.1016/j.compag.2017.12.014).
- Li, H.Z., Zhao, B.C., Guo, G.L. et al. (2018). The influence of an abandoned goaf on surface subsidence in an adjacent working coal face: a prediction method. *Bulletin of Engineering Geology and the Environment*, 77, 305–315.
- Liu, W., Zhang, X., Li, S. et al. (2010). Reasoning about cardinal directions between extended objects. *Artif. Intell.*, 174(12-13), 951–983.
- Mackness, W.A., Ruas, A., and Sarjakoski, L.T. (2011). *Generalisation of Geographic Information: Cartographic Modelling and Applications*. Elsevier.
- Maling, D.H. (2016). *Measurements from Maps: Principles and Methods of Cartometry*. Butterworth-Heinemann.
- Manjunatha, A., Anik, A.R., Speelman, S. et al. (2013). Impact of land fragmentation, farm size, Land ownership and crop diversity on profit and efficiency of irrigated farms in India. *Land Use Policy*, 31, 397–405.
- Molano, R., Rodríguez, P.G., Caro, A. et al. (2012). Finding the largest area rectangle of arbitrary orientation in a closed contour. *Appl. Math. Comput.*, 218(19), 9866–9874.
- Müller, J.C., Lagrange, J.P., and Weibel, R. (1995). *GIS and generalization. Methodology and practice*. London: Taylor and Francis.
- Peng, S.S. (1986). *Coal mine ground control*. John Wiley & Sons.
- Peura, M., and Iivarinen, J. (1997). *Efficiency of Simple Shape Descriptors*. In: 3rd International Workshop on Visual Form. Capri. Italy.
- Pilkey, W.D. (1993). *Formulas for Stress, Strain, and Structural Matrices*. New York: John Wiley & Sons.
- Prokop, J. and Reeves, A.P. (1992). A survey of moment-based techniques for unoccluded object representation and recognition. *Computer Vision. Graphics and Image Processing*, 54(5), 438–460.
- Rosin, P.L. (1999). Measuring rectangularity. *Mach. Vis. Appl.*, 11(4), 191–196.
- Rosin, P.L. (2003). Measuring shape: ellipticity, rectangularity and triangularity. *Mach. Vis. Appl.*, 14(3), 172–184.
- Salishchev, K.A. (1976). *Kartovedeniye*. Moscow University.
- Sarkar, A., Biswas, A., Dutt, M. et al. (2018). Finding a largest rectangle inside a digital object and rectangularization. *J. Comput. Syst. Sci.*, 95, 204–217. DOI: [10.1016/j.jcss.2017.05.006](https://doi.org/10.1016/j.jcss.2017.05.006).

- Smith, J.R., and Chang, S.F. (1996). *VisualSEEK: a fully automated content-based image query system*. In Proceedings of the fourth ACM international conference on Multimedia. Boston, Massachusetts, USA, 87–98.
- Touya, G. (2019). Finding the Oasis in the Desert Fog? Understanding Multi- Scale Map Reading. Proceedings of the ICA workshop on abstraction, scale and perception. Tokyo, Japan.
- Wawer, R., and Nowocień, E. (2018). Water and wind erosion in Poland. *Studia i Raporty IUNG-PIB*. Vol. 58(12) pp. 57–79. (in Polish)
- Weibel, R. (1997). Generalization of spatial data: Principles and selected algorithms. In eds. van Kreveld, M., Nievergelt, J., Roos, T., Widmayer, P. *Algorithmic Foundations of Geographic Information Systems*. Lecture Notes in Computer Science, 1340. Springer.
- White, C. L., and Renner, G. T. (1957). *Natural environment and human Society*. New York, 590–599.
- Woch, F. (2008). Soil protection from erosion in countryside development in Poland. *Nat. Environ. Monitoring*, 9, 79–87.
- Zandonadi, R.S., Luck, J.D., Stombaugh, T.S. et al. (2013). Evaluating field shape descriptors for estimating off-target application area in agricultural fields. *Comput. Electron. Agric.*, 96, 216–226.